



# Mono-model Gramian constrained multi-physics inversion of EM data

**Jide Nosakare Ogunbo**

Brain Korea Professor

Seoul National University, South Korea

EMinar Presentation

5<sup>th</sup> of January, 2022





# 서울대학교 공과대학 에너지자원공학과

Department of Energy Resources Engineering



<https://ere.snu.ac.kr>

# CONTENTS

- **Introduction**
  - Inversion
    - Challenges: existence, stability and uniqueness
- **Multi-physics inversion philosophy implementation**
  - Multi- and Mono-model multi-physics inversions
- **Gramian constrained multi-physics inversion**
  - Synthetic example
  - Field example
    - Bookpurnong airborne time and frequency domain EM data
- **Conclusions**





I

# Introduction

Challenges inherent in inversion



## 2 Basic geophysical preoccupations

- Basically

- Modeling

- Inversion

Table 1: Modeling and Inversion with their issues

Procedure	In Control	Operator	Output
Modeling	Parameters	Forward Operator	Data
Inversion	Data	Inverse Operator	Parameters

Procedure	Associated Cost Issues		
Modeling	Computational Efficiency	Accuracy improvement	
Inversion	Existence	Stability	Uniqueness

# My contemplation today in inversion constituency: ill-posed problems

- Fundamental issues/question (Zhdanov, 2015)
- **Existence/non-existence**
  - Does a solution exist, first question? Deals mathematical formulation of the inverse problem
  - Physical point of view: there should be real geological structures
  - Mathematical view: no adequate numerical model fit observed **noisy** data
  - Noise in the data has no common ground with geophysical field equations.
- **Stability/Instability**
  - If a small perturbation of data gives arbitrary large perturbation of the solution=**Unstable**
- **Uniqueness/non-uniqueness**
  - Non-uniqueness (seems to be inherent problem):
  - A situation where two or more different models/sources sources fit the same data
  - Jackson (1972): inaccurate, insufficient, inconsistent data lead to non-uniqueness
- **Ill-posed inversion problem**
  - With any of these problems occurs, the inverse problem is **ill-posed**.
  - **And how do we solve an ill-posed problem?**

# Practical existence (Zhdanov, 2015)

- **Existence**

- Noise cannot be described by the same operator for data
- No need to completely fit the noisy data
- Hence ***Practical Existence*** is possible where data is fitted within **measurement error bound**
- Solution to non-existence problem is understandably by ***practical existence***.



# Tikhonov Regularization Theory

- **Stability**
- Mathematically speaking, instability occurs when the **inverse operator is not continuous**, making the inverse problem ill-posed.
- Stabilizer main application is to
  - select from the set of possible solutions
  - The solutions that continuously depend on the data
  - and which possesses a specific property depending on the choice of stabilizer
- **The solution to instability is regularization**,
  - which conditions an ill-posed problem to a well-posed problem, making the inverse operator continuous.
  - Regularization algorithm aims to consider, instead of one ill-posed (unregularized) inverse problem, a family of well-posed problems.



# Regularized inversion

- To stabilize such an inversion, a regularized parametric functional can be written as linear combination of the misfit and stabilizing functionals (Zhdanov, 2015)

$$P^\alpha(m) = \mu_D + \alpha s(m), \quad (1)$$

- where  $P^\alpha(m)$  is the Tikhonov parametric functional for model parameter  $m$ ;  $\mu_D$  is the misfit functional,  $s(m)$  is the stabilizing functional
- And to solve for the model parameter  $m$

$$P^\alpha(m) = \min. \quad (2)$$

# Practical uniqueness

- **Uniqueness**

- There are uniqueness theories that work for only certain geophysical models.
- Uniqueness theories are limited to certain geophysical models
- ***Practical uniqueness*** is proposed by Zhdanov (2015),
  - where the geometrical dimension for data acquisition is at least the same as that for inverted models e.g. 3D for both data and model;
  - but if the data dimension is 4D for 3D model, that is even better.



II



# Multi-physics inversion Philosophy implementation

Multi-modal, Mono-model multi-physics inversion



# Multi-physics/joint inversion tackle non-uniqueness

- The **practical uniqueness is not the general solution** to non-uniqueness problem as it is restrictive and costly
- However, recently, researchers have attempted to tackle the non-uniqueness problem by joint inversion of
  - Multiple data sets
  - Multiple geophysical approaches/techniques of methods
- For  $n$  data sets and model parameters, a third term (coupling term) will be added to the Tikhonov Parametric Functional in equation (1), with the basic form given as:

$$P^\alpha(m^i) = \sum_{i=1}^n \mu_D^i + \alpha \sum_{i=1}^n s^i(m^i) + \beta \sum_{i=1}^n c(m^1, m^2, \dots, m^n) \quad (3)$$

Where  $c$  is a general representation of the joint inversion or multi-physics constraints or coupling term, weighted by  $\beta$ .

# Some multi-physics constraints

- Constraints help to couple certain feature between interacting models and/or data.
- There is a growing list, but only a few will be mentioned here
- **Cross-gradient**
  - Popular and useful where physical properties are not correlated but nevertheless have similar structural constraints)
- **Petrophysical relations**
- **Fuzzy c-means**
- **Gramian**
  - Minimization of the determinant of the Gram matrix

# Implementation of joint inversion within its philosophy

Table 2: Multi-modal and mono-model multi-physics inversion

Joint inversion	Data/approach	Model	Reference
<b>Mono-model</b>	<b>Similar</b> (DC, EM)	<b>Same</b> (resistivity)	Vozoff and Jupp (1975)
<b>Mono-model</b>	<b>Multiple approaches</b> on <i>same data set</i> (refraction travelttime migration and tomography)	<b>Same</b> (velocity)	Zhang (1997)
<b>Multi-modal</b>	<b>Different</b> (seismic and EM)	<b>Different</b> (velocity and resistivity)	Ogunbo et al. (2018)

# Multi-modal joint inversion (a few examples)

**Table 3: Multi-modal multi-physics inversion examples**

Authors	Method 1	Method 2	Constraint
Gallardo and Meju (2003; 2004)	DC resistivity	Seismic travelttime	Cross-gradient
Ogunbo et al. (2018)	Seismic travelttime	Electromagnetic	Cross-gradient
Hu et al. (2009)	EM	Seismic	Cross-gradient
Carter-McAuslan et al. (2015)	Seismic tomography	Gravity	Fuzzy c-means
Gao et al. (2010; 2012)	EM	Full waveform seismic	Petrophysical
Abubakar et al. (2012)	CSEM	Seismic full waveform	Petrophysical
Zhdanov et al. (2012)	Gravity	Magnetic	Gramian
Zhu et al. (2013)	Airborne Gravity	Magnetic	Gramian

Authors	Method 1	Method 2	Method 3	Constraints
Moorkamp et al. (2011)	MT	Gravity	Seismic refraction	Mathematical relation; Cross-gradient

# Mono-model joint inversion

Table 4: Mono-model multi-physics inversion examples

Authors	Method 1	Method 2	Constraint	Remark
Vozoff and Jupp (1975)	DC resistivity	Magnetotelluric	None	
Raiche et al. (1985)	TEM	Schlumberger DC	None	
Sunwall et al. (2013)	Time-domain AEM	Frequency-domain AEM	None	Deep and shallow Resolution complements
Ogunbo (2019)	Time-domain AEM	Frequency-domain AEM	Gramian	
Ogunbo et al. (2020)	Gravity	Magnetic	Gramian	Inverting coincident geometry
Ogunbo et al. (2021)	Gravity	First horizontal derivative of Gravity	Gramian	Inverting coincident geometry

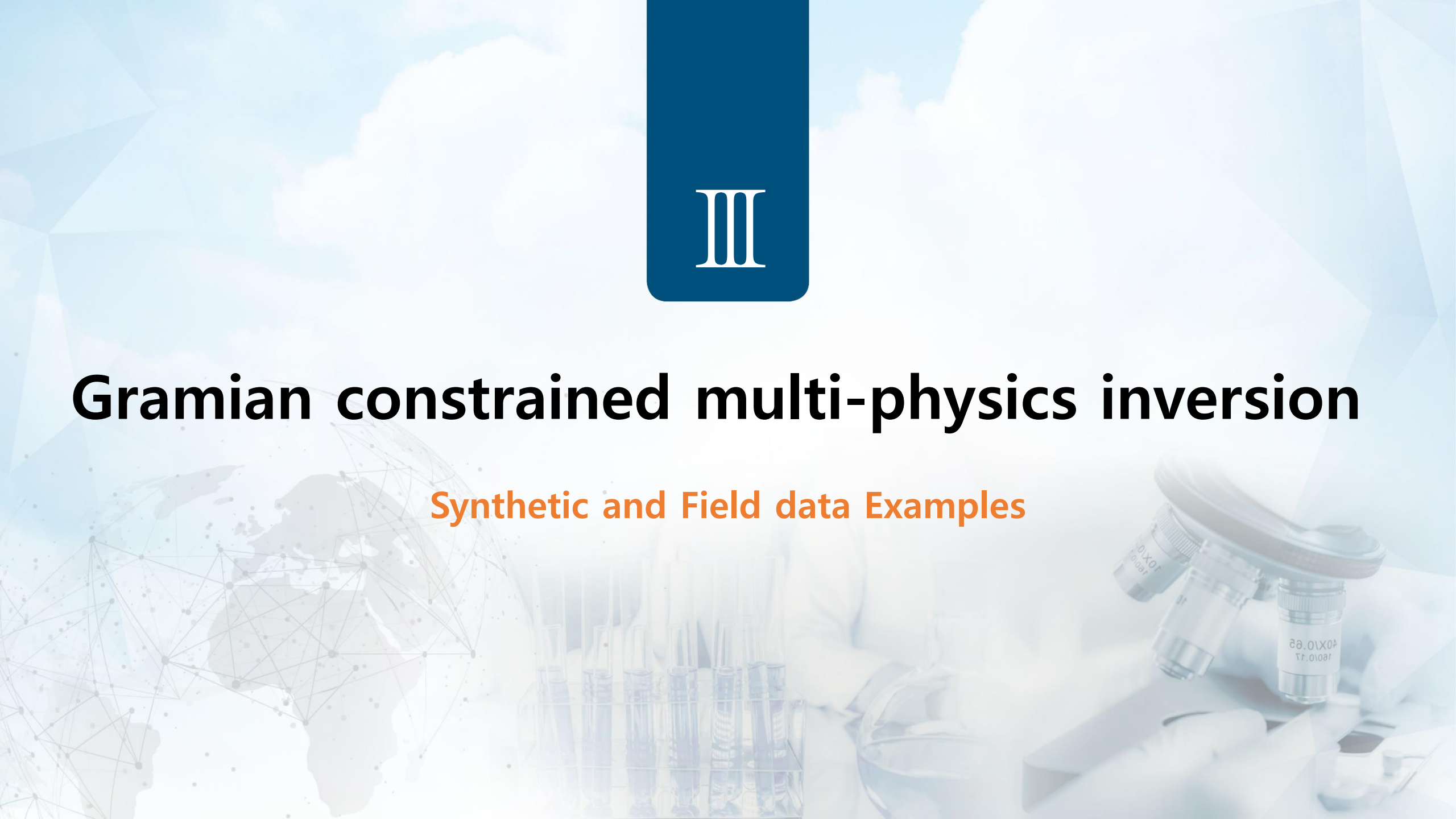
Although there are several applications of the mono-model Gramian constrained joint inversion that I have worked on, I present results from EM-EM case from Ogunbo (2019)





# Gramian constrained multi-physics inversion

Synthetic and Field data Examples



# Results from Ogunbo (2019)

## Earth and Space Science



### RESEARCH ARTICLE


10.1029/2019EA000605

#### Key Points:

- The gramian-constrained joint inversion of RESOLVE and SkyTEM data of salinized Bookpurnong Irrigation District, South Australia is performed
- The Gramian constraint exploits the linear correlation and enforces it between similar methods
- The correlation coefficient is an additional measure of confidence on the inverted results

Correspondence to:

## Mono-Model Parameter Joint Inversion by Gramian Constraints: EM Methods Examples

J. N. Ogunbo<sup>1,2</sup> 

<sup>1</sup>Department of Applied Geophysics, The Federal University of Technology, Akure, Nigeria, <sup>2</sup>Formerly at Earth Resources Lab, Massachusetts Institute of Technology, Cambridge, MA, USA

---

**Abstract** Joint inversions of coincident geophysical data are usually constrained to produce more reliable subsurface models. Structural, petrophysical, model parameter correlation, empirical, and transforms are some of the published constraints. The Gramian constraint provides a broad mathematical framework for implementing the aforementioned constraints. The Gramian constraint is formed from the determinant of the inner products of the model parameters involved. Previous works have used the Gramian constraint to invert multimodal parameters of different geophysical methods. But there has not been any extension of Gramian-constrained joint inversion to mono-model parameter from similar geophysical

# Gramian constrained joint inversion (Yue et al., 2013)

- Operator relationships between multiple data sets and model parameters is given as

$$d^i = A^i(m^i) \quad i = 1, 2, 3, \dots, n, \quad (4)$$

where  $A^i$  are the nonlinear forward operators;  $d^i$  are the different observed data sets, and  $m^i$  are the model parameters

For convenience, we can use the dimensionless weighted model parameters

$$\tilde{m}^i = W_m^i m^i, \quad (5)$$

$W_m^i$  is the corresponding linear operator of model weighting (Zhdanov, 2015)

# Gramian constrained joint inversion (Yue et al., 2013)

- The Gramian of a system of model parameters  $(\tilde{m}^1, \tilde{m}^2, \dots, \tilde{m}^{n-1}, \tilde{m}^n)$  is the determinant,  $G(\tilde{m}^1, \tilde{m}^2, \dots, \tilde{m}^{n-1}, \tilde{m}^n)$ , of the Gram matrix of a set of functions,  $(\tilde{m}^1, \tilde{m}^2, \dots, \tilde{m}^{n-1}, \tilde{m}^n)$ , defined as:

$$G(\tilde{m}^1, \tilde{m}^2, \dots, \tilde{m}^{n-1}, \tilde{m}^n) = \begin{vmatrix} \langle \tilde{m}^1, \tilde{m}^1 \rangle & \langle \tilde{m}^1, \tilde{m}^2 \rangle & \dots & \langle \tilde{m}^1, \tilde{m}^n \rangle \\ \langle \tilde{m}^2, \tilde{m}^1 \rangle & \langle \tilde{m}^2, \tilde{m}^2 \rangle & \dots & \langle \tilde{m}^2, \tilde{m}^n \rangle \\ \dots & \dots & \dots & \dots \\ \langle \tilde{m}^n, \tilde{m}^1 \rangle & \langle \tilde{m}^n, \tilde{m}^2 \rangle & \dots & \langle \tilde{m}^n, \tilde{m}^n \rangle \end{vmatrix}, \quad (6)$$

- where  $\langle \tilde{m}^1, \tilde{m}^2 \rangle$  is the dot product of  $\tilde{m}^1$  and  $\tilde{m}^2$
- The Gramian provides a measure of correlation between the different model parameters or their attributes
- By imposing additional requirement of the minimum of the Gramian in the regularized inversion, we generally obtain multimodal inverse solutions with enhanced correlations between the different model parameters or attributes

# Method: Gramian constrained joint inversion

- Adapting the general formulation to the case of 2 different types of EM methods
- Taking  $m_1$  and  $m_2$  as the logarithm of resistivity of time and frequency domain airborne EM data respectively, the **Gram matrix is formed from the dot**  $m_1$ , and  $m_2$  (Zhdanov, 2015):
- The parametric functional to minimize with the Gramian stabilizer is (Zhdanov, 2015; Ogunbo, 2019):

$$P^\alpha(\tilde{m}^1, \tilde{m}^2) = \sum_{i=1}^2 (\|(\tilde{A}^i(\tilde{m}^i) - \tilde{d}^i)\|^2) + \alpha \sum_{i=1}^2 S_{MN,MS,MGS}^i + \beta \sum_{i=1}^2 G(m_1, m_2), \quad (7)$$

where  $\tilde{A}^i(\tilde{m}^i)$  are weighted predicted data;  $S_{MN}^i$ ,  $S_{MS}^i$ ,  $S_{MGS}^i$  are the stabilizing functionals based on the minimum norm, minimum support and minimum gradient supports respectively

$\alpha$  is the regularization parameter, and  $\beta$  is the weight for the Gramian stabilizer.

We minimize equation (7) and solve by iterative regularized conjugate gradient method. Details are found in Zhdanov (2015).

# Synthetic Example: Imaging Resistivity blocks

- Resistivity structure in Figure 1 has of 500 Ohm-m and 30 Ohm-m buried in a background resistivity of 100 Ohm-m.
- **Methods** used are
  - Time domain airborne EM (TDAEM)
  - Frequency domain airborne EM (FDAEM)
- **RESOLVE system is used to acquire FDAEM**
  - Flown at altitude of 20 m with horizontal receiver offset of 7.93 m.
  - Acquires horizontal coplanar in-phase and quadrature responses at 5 frequencies
- **SkyTEM is used to acquire TDAEM**
  - Flown at an altitude of 40.55 m, station spacing of 13.26 m; offtime 4.167 ms.

The resistivity model has 7 data points.  
Number of layers is 6 and the Layer thickness is 5 m

10 stand-alone iterations preceding joint inversion.  
Noise levels: 0%, 1%, 3%, to check the robustness of the results

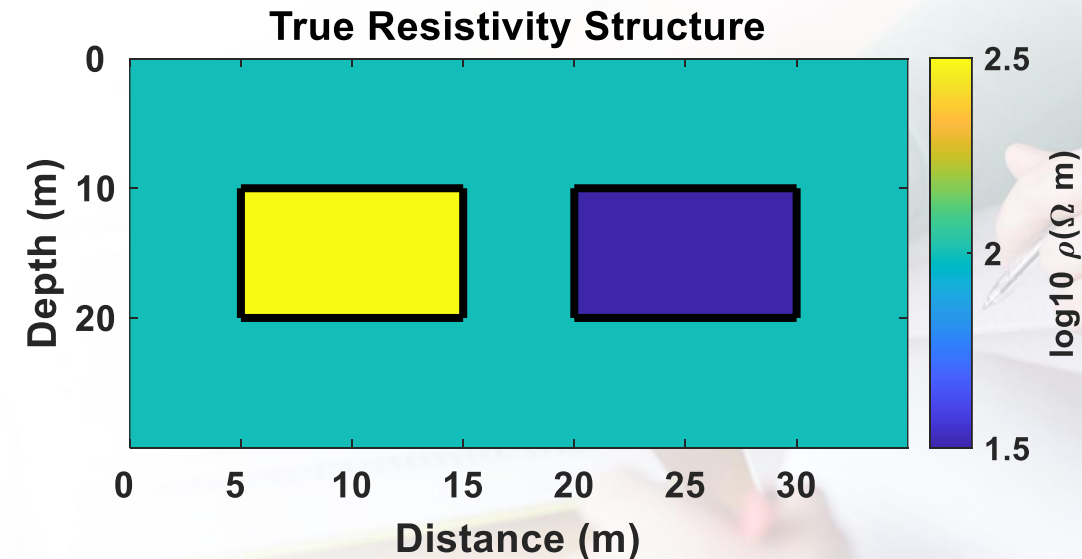
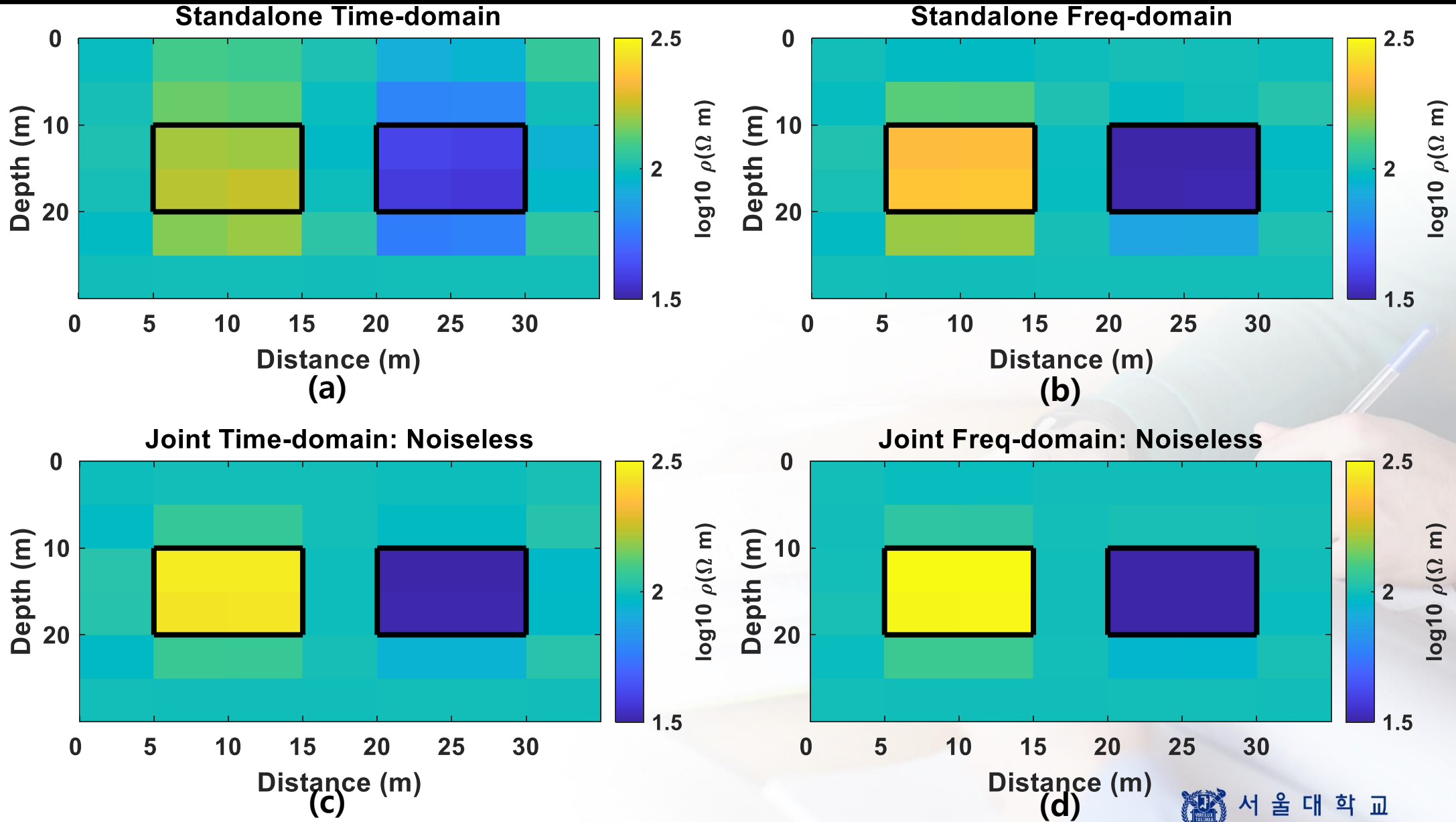


Figure 1: True synthetic resistivity model

# Results: Standalone and Noiseless Joint inversion



Difficult to choose which standalone result is representative of true model.

There is a high correlation between the jointly inverted models, helping

Figure 2: Inverted resistivity models (a) and (b) are the standalone time- and frequency-domain respectively; (c) and (d) are the corresponding jointly inverted resistivity models for noiseless data

# Joint inversion: high correlation even up to 3 % noise

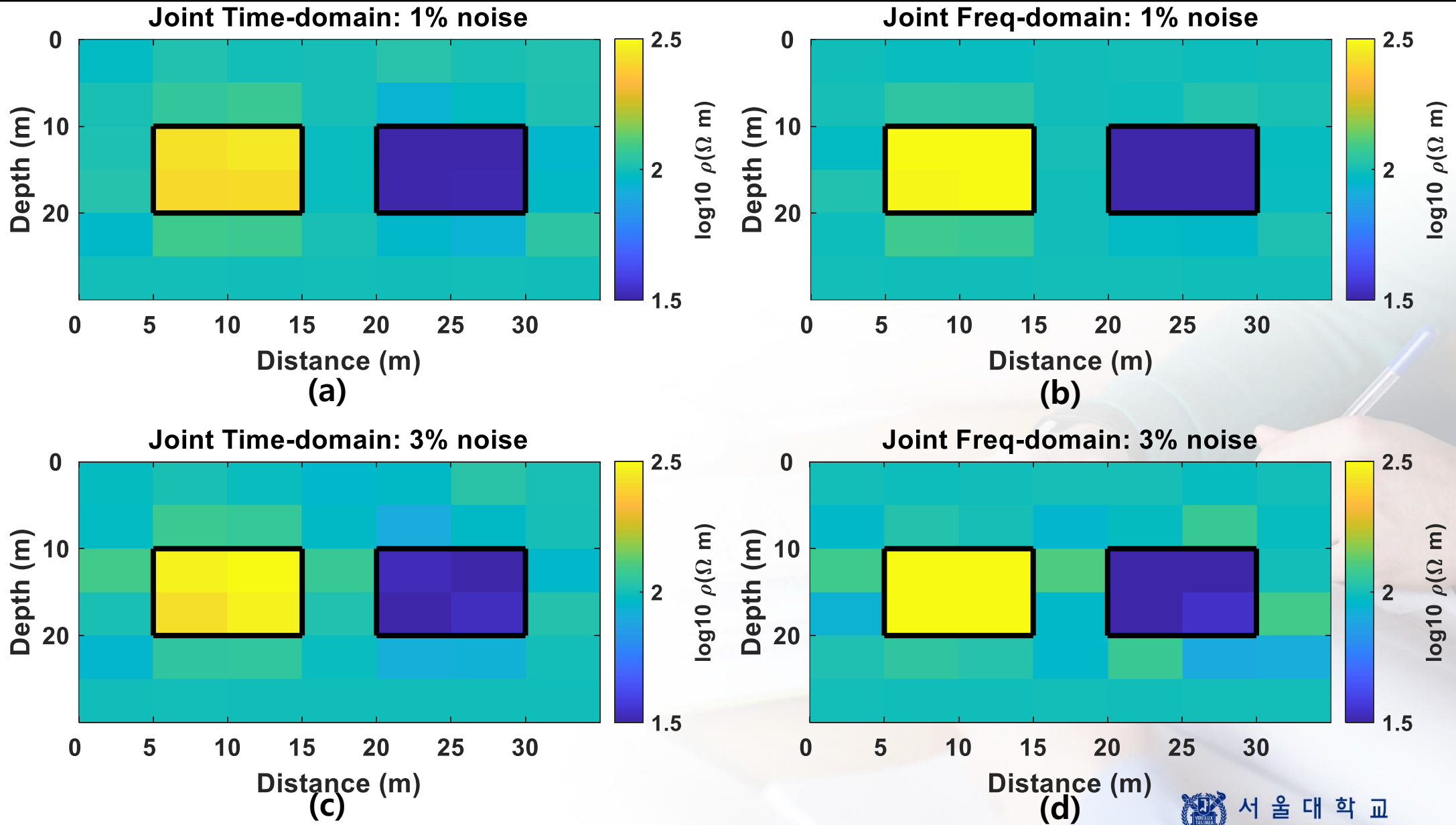
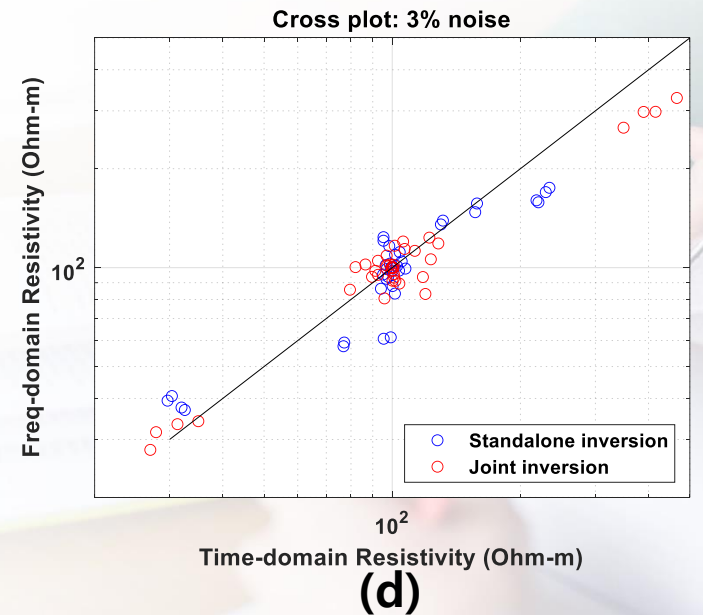
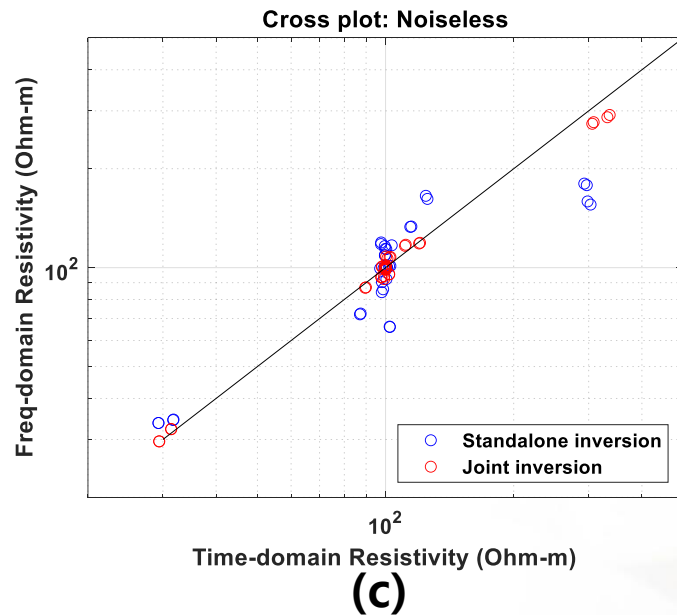
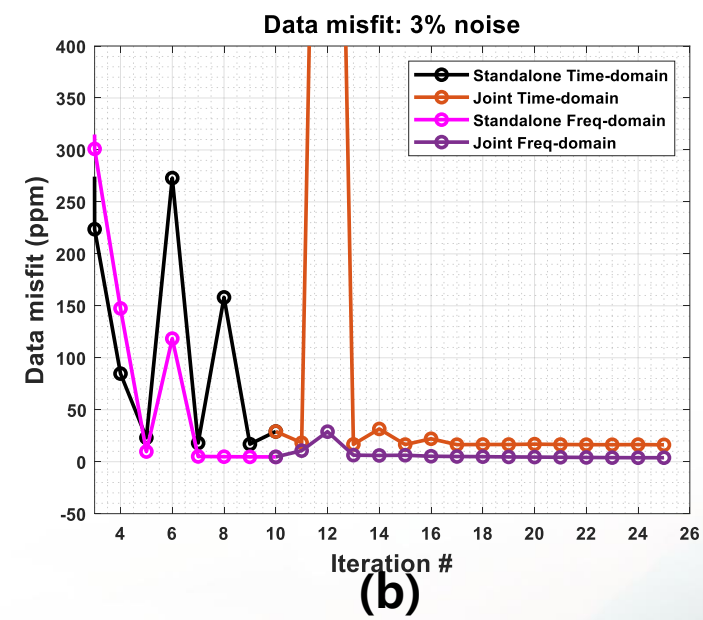
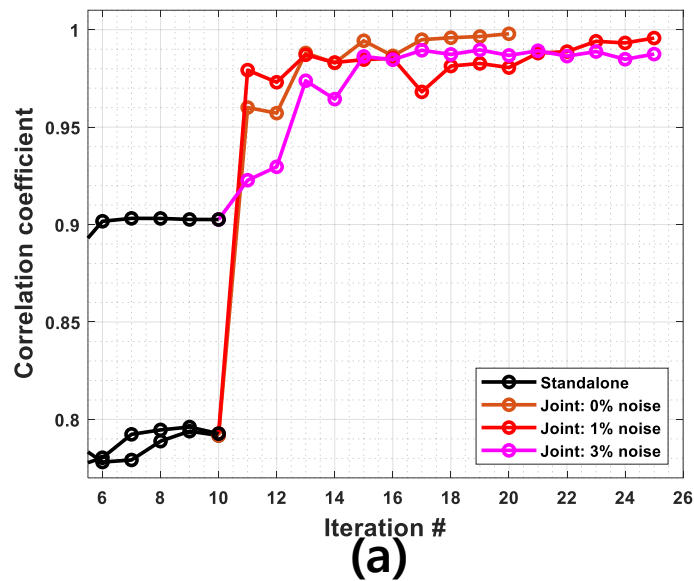


Figure 3: Jointly inverted resistivity models for (a) and (b) 1% noisy time- and frequency-domain data respectively; (c) and (d) are the corresponding inverted resistivity models for 3% noisy data



# Correlation coefficient, convergence, cross plots, plots with iterations



We observe that the Gramian constraint indeed increases the correlation coefficient between the jointly inverted resistivity models; although higher noise percentage has lower correlation coefficient value; while the data misfit reduces and the result approach the true solution;

Figure 4: (a) Correlation coefficient; (b) data misfit for 3% noisy data; cross plots of jointly inverted resistivity models (c) from noiseless data and (d) from 3% noisy data

# Data fit for the Synthetic Airborne EM data overlay

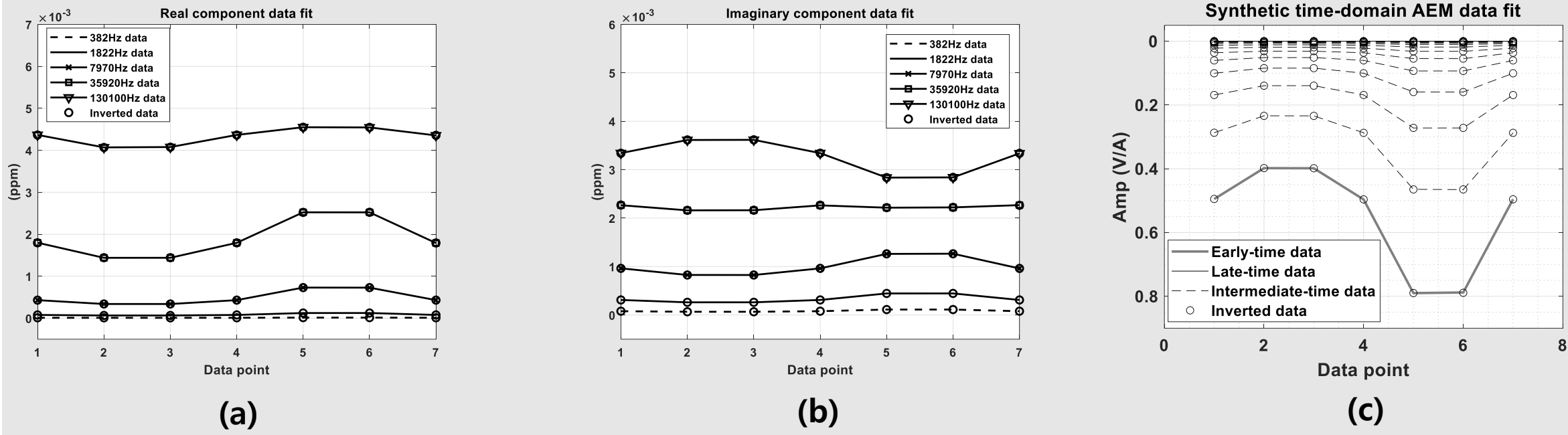


Figure 5: Synthetic data fit for (a) real component (b) imaginary component of the frequency-domain AEM data; (c) time-domain data

# Field EM Data: Bookpurnong Irrigation District

- **RESOLVE system (FDAEM)**

- Flown at altitude of 33.46 m with horizontal receiver offset of 7.86 m.
- Acquires horizontal coplanar in-phase and quadrature responses at 5 frequencies

- **High Moment SkyTEM (TDAEM)**

- Flown at an altitude of 39.8 m, horizontal receiver offset of 12.4 m; offtime 4.167 ms.

- **Methods** used are

- Time domain airborne EM (TDAEM)
- Frequency domain airborne EM (FDAEM)

- Data acquired over the highly salinized Bookpurnong Irrigation District, South Australia. TDAEM in 2006; FDAEM in 2008 : 2 years time lapse

- The resistivity model has 10 data points.

- Number of layers is 14.

- 6 stand-alone iterations preceding 10 joint inversion iterations.

# Results: Standalone and joint inversion results

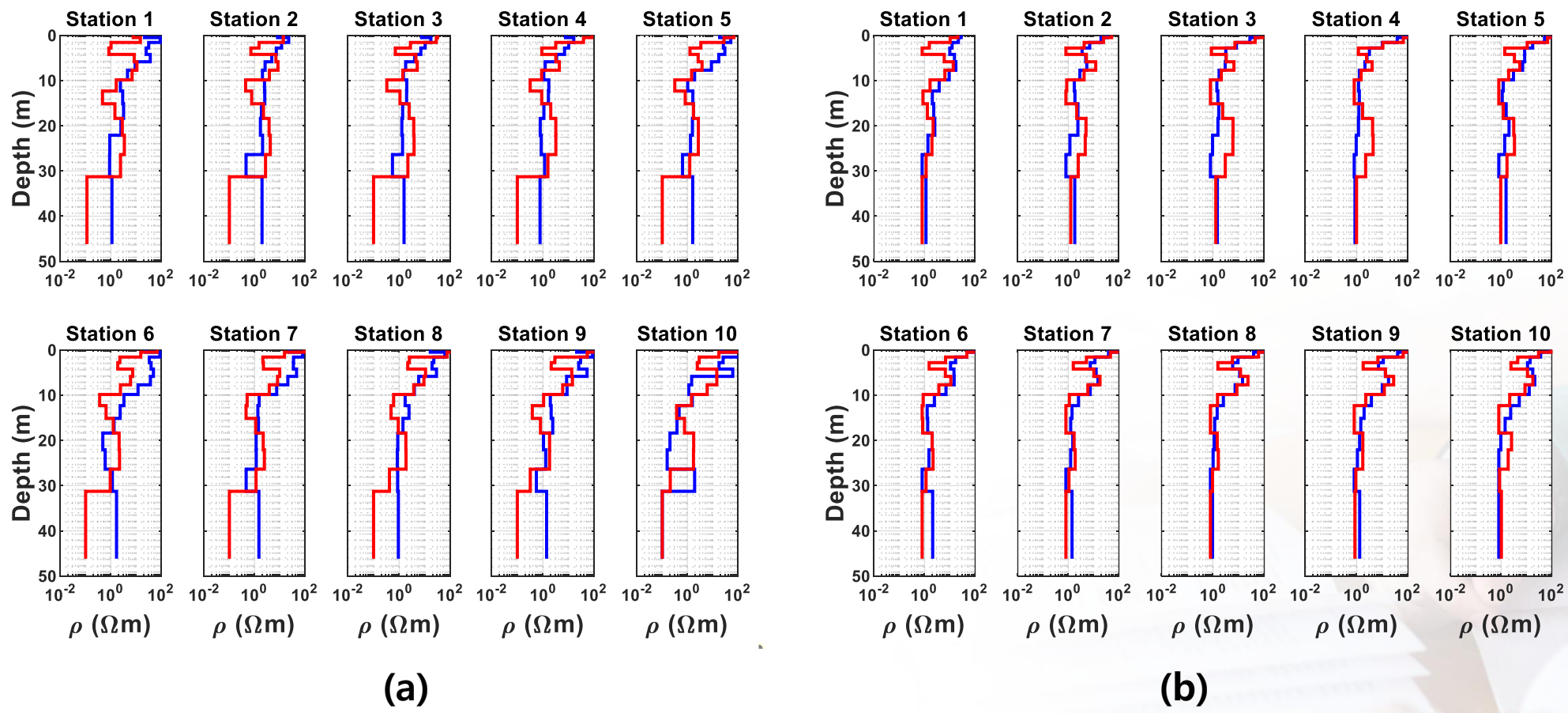
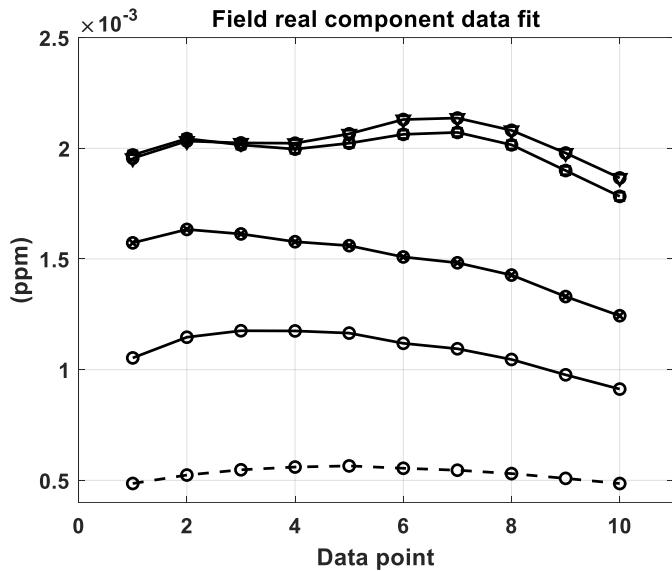


**Figure 6: resistivity models from the (a) standalone inversion with visible weak correlation between the resistivity models from the frequency-domain (red) and time-domain (blue) data. (b) joint inversion results constrained by the Gramian constraint. It is apparent that the Gramian constraint synergizes the inversion towards a common unique result (Results from Ogunbo, 2019).**

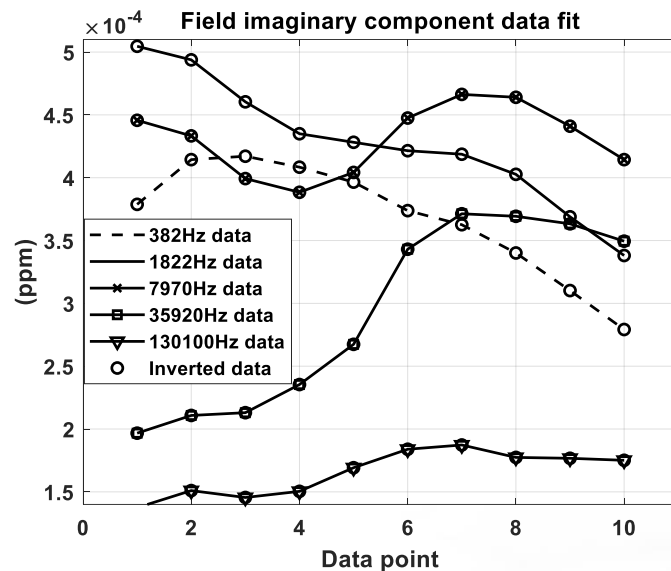
The joint inversion results suggest that at the Bookpurno ng Irrigation District has a background resistivity of 1  $\Omega\text{m}$  which is still largely unaffected by the salinization from 20 m depth. However, in the near-surface the salinization over the two-year time lapse has increased the conductivity (decreased resistivity) as captured by the jointly inverted resistivity model from the frequency-domain data.

In the standalone results, neither the time- nor the frequency domain resistivity models can be confidently used as the final resistivity models; however, Gramian constraint enforces the correlation between the resistivity models, to focus the solution towards high confident interpretation.

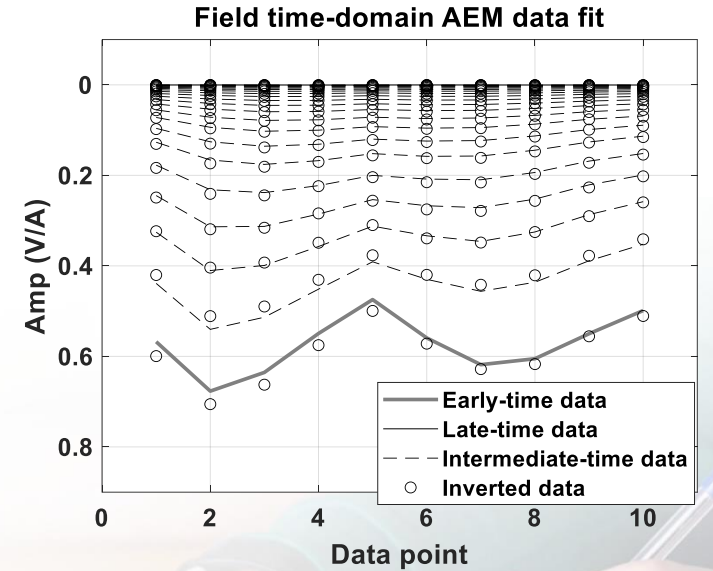
# Field data fit



(a)



(b)



(c)

Figure 7: Field data fit for (a) real component (b) imaginary component of the frequency-domain AEM data;

# Field data: data misfit, correlation coefficient, cross plot

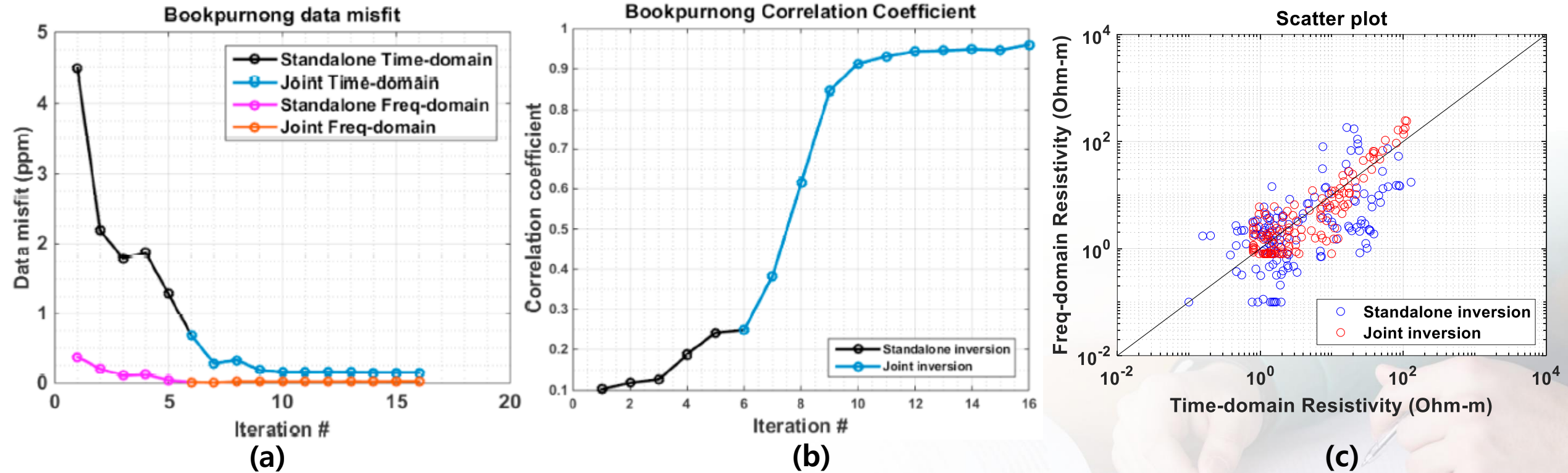


Figure 8: (a) RMSE with iteration (b) correlation coefficient with iteration (c) and cross plot of jointly inverted resistivity models

# IV

## Conclusions



# Conclusions

- The multi-physics from the frequency and time-domain airborne EM (AEM) data has been jointly inverted with the Gramian constraint, which is the dot product of two resistivity model vectors.
- The Gramian constraints synergize the linear correlation between the resistivity models to produce more reliable images than those from the standalone inversions.
- The application of the concept on synthetic data proves the compelling role of the Gramian influence in the joint inversion even in the presence of noise. Increasing linear correlation coefficient and decreasing data misfit with iteration is further ensured by the Gramian constraint.
- Moreover, the frequency and time-domain AEM data from Bookpurnong Irrigation District, South Australia have been jointly inverted with Gramian constraint which reveals a resistivity background of  $1 \Omega\text{m}$  with a salinized (lower resistivity values) near surface (shallow depths).



# References

- Abubakar, A., Gao, G., Habashy, T. M., & Liu, J. (2012). Joint inversion approaches for geophysical electromagnetic and elastic fullwaveform data. *Inverse Problems*, 28(5). <https://doi.org/10.1088/0266-5611/28/5/055016>
- Carter-McAuslan, A., Lelièvre, P. G., & Farquharson, C. G. (2015). A study of fuzzy c-means coupling for joint inversion, using seismic tomography and gravity data test scenarios. *Geophysics*, 80(1), W1–W15. <https://doi.org/10.1190/geo2014-0056.1>.
- Gallardo L. A., and Meju, M. A. (2003) Characterization of heterogeneous near-surface materials by joint 2D inversion of dc resistivity and seismic data. *Geophysical Research Letters*, **30**, 1658, doi:10.1029/2003GL017379.
- Gallardo, L. A., & Meju, M. A. (2004). Joint two-dimensional DC resistivity and seismic travel time inversion with cross-gradients constraints. *Journal of Geophysical Research*, 109, B03311. <https://doi.org/10.1029/2003JB002716>
- Gao, G., Abubakar, A., & Habashy, T. M. (2010). Simultaneous joint petrophysical inversion of electromagnetic and seismic measurements. *SEG Technical Program Expanded Abstracts*, 2010, 2799–2804. <https://doi.org/10.1190/1.3513425>
- Gao, G., Abubakar, A., & Habashy, T. M. (2012). Joint petrophysical inversion of electromagnetic and full-waveform seismic data. *Geophysics*, 77(3), WA3–WA18. <https://doi.org/10.1190/GEO2011-0157.1>

# References

- Hu, W., Abubakar, A., & Habashy, T. M. (2009). Joint electromagnetic and seismic inversion using structural constraints. *Geophysics*, 74(6), R99–R109. <https://doi.org/10.1190/1.3246586>
- Jackson, D. D. (1972). Interpretation of inaccurate, insufficient and inconsistent data. *Geophysical Journal of the Royal Astronomical Society*, 28(2), 97–109. <https://doi.org/10.1111/j.1365-246X.1972.tb06115.x>
- Moorkamp, M., Heincke, B., Jegen, M., Roberts, A.W., and Hobbs R.W. (2011) A framework for 3-D joint inversion of MT, gravity and seismic refraction data. *Geophysical Journal International*, **184**, 477-493.
- Ogunbo, J. N. (2019) Mono-model parameter joint inversion by Gramian constraints: EM methods examples. *Earth and Space Science*, **6**, 741-751, <https://doi.org/10.1029/2019EA000605>.
- Ogunbo, J. N., Marquis, G., Zhang, J., & Wang, W. (2018). Joint inversion of seismic traveltimes and frequency-domain airborne electromagnetic data for hydrocarbon exploration. *Geophysics*, 83(2), 1–79. <https://doi.org/10.1190/geo2017-0112.1>
- Ogunbo, J. N., Amigun, J. O., Oluwadare, O. A., Olowokere, M. T., Fadugba, O. I., and Shin, C. (2020). Multi-physics inversion of common density-susceptibility geometry constrained by the Gramian. *SEG Technical Program Expanded Abstracts*, 2020, 989-993. <https://doi.org/10.1190/segam2020-3415790.1>
- Ogunbo, J. N., Min, D.-J., Shin, C., and Ojo, B. T. (2021), Multi-physics inversion of coincident geometrical coordinates from the gravity and its first horizontal data. *SEG Technical Program Expanded Abstracts*, 2021, 1761-1765. <https://doi.org/10.1190/segam2021-3582621.1>

# References

- Raiche, A. P., Jupp, D. L. B., Rutter, H., & Vozoff, K. (1985). The joint use of coincident loop transient electro magnetic and Schlumberger sounding to resolve layered structures. *Geophysics*, 50(10), 1618–1627. <https://doi.org/10.1190/1.1441851>
- Sunwall, D., Cox, L., & Zhdanov, M. (2013). Joint 3D inversion of time- and frequency domain airborne electromagnetic data. *SEG Technical Program Expanded Abstracts*, 2013, 713–717. <https://doi.org/10.1190/segam2013-0711.1>
- Vozoff, K., & Jupp, D. L. B. (1975). Joint inversion of geophysical data. *Geophysical Journal of the Royal Astronomical Society*, 42(3), 977–991. <https://doi.org/10.1111/j.1365-246X.1975.tb06462.x>
- Zhang, J., and Toksöz, M. N. (1997), Joint Refraction Traveltime Migration and Tomography. *Symposium on the Application of Geophysics to Engineering and Environmental Problems Proceedings* : 901-910.
- <https://doi.org/10.4133/1.2922471>
- Zhdanov, M. S. (2015). *Inverse theory and applications in geophysics* (2nd ed., pp. 730). Amsterdam: Elsevier. ISBN-978-0-444-62674-5
- Zhdanov, M. S., Gribenko, A., & Wilson, G. (2012). Generalized joint inversion of multimodal geophysical data using Gramian constraints. *Geophysical Research Letters*, 39, L09301. <https://doi.org/10.1029/2012GL051233>
- Zhu, Y., Zhdanov, M. S., & Čuma, M. (2013). Gramian constraints in the joint inversion of airborne gravity gradiometry and magnetic data. *SEG Technical Program Expanded Abstracts*, 2013, 1166–1170. <https://doi.org/10.1190/segam2013-0735.1>



# Acknowledgement

I acknowledge the support by the Brain Korea 21 FOUR Program  
(No. 4199990314119)

Data source acknowledged: made accessible by CSIRO (<https://doi.org/10.6084/m9.figshare.5107711>)

Thank you for listening